

# Hydrogen sensor based on thin film nanocrystalline n-GaN/Pd Schottky diode

S N Das and A K Pal<sup>1</sup>

Department of Instrumentation Science, USIC Building, Jadavpur University,  
Calcutta 700 032, India

E-mail: [msakp2002@yahoo.co.in](mailto:msakp2002@yahoo.co.in)

Received 18 August 2007, in final form 16 September 2007

Published 16 November 2007

Online at [stacks.iop.org/JPhysD/40/7291](http://stacks.iop.org/JPhysD/40/7291)

## Abstract

Nanocrystalline n-GaN in thin film form was deposited onto fused silica substrates by high pressure dc sputtering of Si(1 at%) doped GaN target. An Al/n-GaN/Pd Schottky diode was realized by depositing n-GaN nanocrystalline layer onto Al-coated fused silica substrate under identical deposition conditions. Top Pd contacts were obtained by evaporating Pd using an appropriate mask. Corresponding current–voltage characteristics of the Schottky diodes were recorded before and after hydrogen gas exposure.  $I$ – $V$  variations were analysed in the light of the existing theories. The ideality factor for the Schottky diodes varied between 3.4 and 4.5. The series resistance of the diode before gas and after gas exposure were found to be  $\sim 500$  k $\Omega$  and  $\sim 300$  k $\Omega$ , respectively. The barrier height could be seen to decrease significantly with increased hydrogen concentration while it increased with temperature.

(Some figures in this article are in colour only in the electronic version)

## 1. Introduction

Growing demands for hydrogen sensors with long-term stability in high temperature operational environments have led to studies on some wide gap semiconductor materials for sensor materials [1–6]. For safety reasons, the determination of hazardous hydrogen concentration in air is an important issue in many areas of industrial applications. Si-based materials (SiC, Pt–SiO<sub>2</sub>–SiC, etc) were studied extensively in the past for fabricating hydrogen gas sensors but these sensors could not sustain high temperature operation due to the inherent problem of silicide formation at  $\sim 673$  K and soldering the contacts [7, 8].

In recent years, gallium nitride has gained increasing attention for use in electronic and opto-electronic devices [9–12]. As a wide gap material, GaN exhibits a high breakdown voltage, a high thermal conductivity and a large saturation electron drift velocity. In addition to the above, high bond strength of the III–V compounds offers high thermal stability for realizing high temperature operative devices. These properties of GaN have ushered the possibility of realizing hydrogen sensors satisfying the stringent conditions of the sensors [2, 3, 13]. Proper combination of metals with

the wide gap GaN, which is chemically resistant to all known aggressive gases in air, was thought to be an ideal answer to the above. Schottky contacts were used as the key element for the device operation controlling the width of the depletion layer as desired. Hydrogen accumulation at the metal/GaN interface would modulate the barrier height of the Schottky contact which in turn would modify the  $I$ – $V$  characteristics and this change may be used to fabricate the requisite hydrogen sensor. In general, bulk GaN epilayers were utilized to study the hydrogen-sensing activity. The preparation of the epilayer involved high cost and intricate deposition procedures. Thus, utilization of GaN in nanocrystalline form having large surface to volume ratio and prepared by a scalable and cost-effective technique would be a welcome proposition for fabricating hydrogen gas sensors with improved performance. There seems to be no report till now on sensors based on GaN in nanocrystalline form.

To the best of our knowledge, the fabrication of Schottky diode structures using GaN in nanocrystalline form has been reported recently by this group [14]. In this communication, we report hydrogen-sensing properties of Schottky diodes (Al/n-GaN/Pd) made out of n-type GaN nanocrystallites in thin film form. Schottky diodes thus formed were characterized by measuring  $I$ – $V$  relationships recorded

<sup>1</sup> Author to whom any correspondence should be addressed.

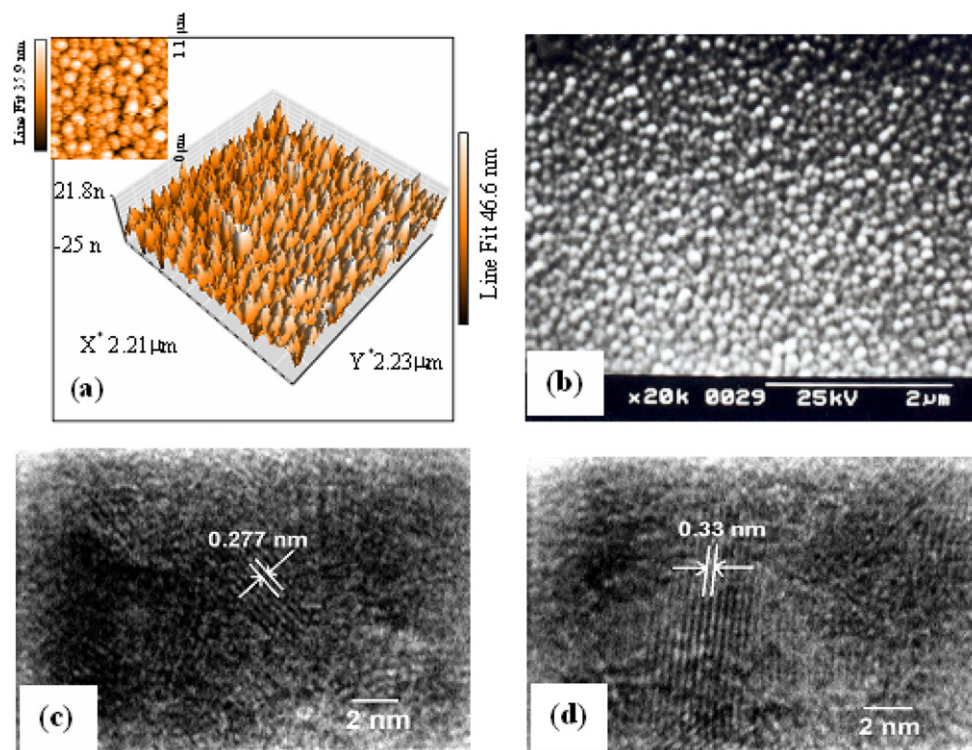


**Figure 1.** (a) AFM and (b) SEM micrographs along with the corresponding HRTEM pictures (c), (d) of a representative n-GaN film deposited at  $T_s = 300$  K and 30 Pa.

at different temperatures before and after hydrogen gas exposure.

## 2. Experimental details

n-GaN in nanocrystalline thin film form was deposited onto fused silica substrates (quartz) by high pressure ( $\sim 30$  Pa) dc sputtering ( $\sim 1.5$  kV;  $5 \text{ mA cm}^{-2}$ ) of a Si(1 at%) doped GaN target in argon plasma at 300 K for a fixed deposition time. The distance between the target (2.5 cm diameter) and substrate was  $\sim 2.5$  cm. The base pressure of the stainless steel sputtering chamber was  $\sim 10^{-6}$  Torr. Schottky diode structures comprising of nanocrystalline Si-doped GaN layers were realized by using a multi-target sputtering unit. For realizing Al/n-GaN/Pd Schottky diodes, n-GaN nanocrystalline layer was deposited onto Al-coated fused silica substrate under identical deposition conditions. An aluminium back contact was deposited by vacuum evaporation at a system pressure  $\sim 10^{-6}$  Torr keeping the substrate temperature at  $\sim 373$  K. The aluminium film was quite adherent and shiny. Top contacts were realized by evaporating Pd using an appropriate mask. The Schottky diodes were then placed on a heavy copper block acting as the sample holder kept inside a test chamber for recording the  $I$ – $V$  relationships at different temperatures before and after hydrogen gas exposure. The test chamber is basically a cylindrical stainless steel chamber having appropriate connectors for evacuation, electrical connectors and gas introduction jigs. A Keithley electrometer (Model 6517A) was used to record the  $I$ – $V$  characteristics. The sample temperature was monitored and controlled by a thermocouple attached to the substrate. A known amount

of hydrogen was injected from an ampoule along with argon gas acting as a diluting agent to get the required percentage (in ppm) of hydrogen in the measuring chamber.

Raman spectra were recorded by using a Renishaw InVia micro-Raman spectrometer using 514 nm argon laser. FTIR spectra were recorded in the range  $400$ – $4000 \text{ cm}^{-1}$  by using a Nicolet<sup>TM</sup>-380 FTIR. It may be noted here that atomic force microscope (AFM), scanning electron microscope (SEM) pictures, Raman and FTIR measurements were recorded on the nanocrystalline GaN films before fabricating the Schottky diodes as it was quite difficult to record the above after completion of the sensing studies. The other details of the experimental technique were given in an earlier communication [14].

## 3. Results and discussion

### 3.1. Microstructural studies

Figures 1(a) and (b) show the AFM and SEM pictures of a representative nanocrystalline n-type GaN film deposited here. One may observe that the films are compact in nature and contained nanocrystallites of n-GaN having an average crystallite size of  $\sim 100$  nm. The 3D AFM picture of the same film indicates (figure 1(a)) that the nanocrystallites are not spherical but resemble hexagonal crystallites grown with  $c$ -axis vertically. The corresponding high-resolution TEM (HRTEM) pictures (figures 1(c) and (d)) of a representative nanocrystalline n-GaN film indicated an interplanar spacing  $\sim 0.277$  nm for (1 0 0) planes of hexagonal n-GaN (figure 1(c)). Figure 1(d) shows the presence of Si in n-GaN with interplanar distance of  $\sim 0.33$  nm for (2 0 0) planes for Si nanocrystallites.

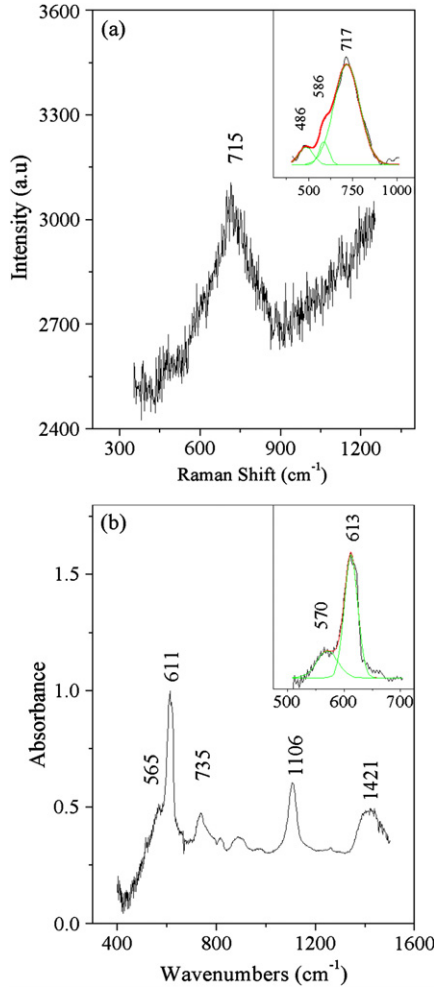


**Figure 2.** (a) Raman spectra, (b) FTIR spectra for a representative n-GaN film.

### 3.2. Raman studies

Raman measurements were carried out to determine the quality of the n-GaN films prepared here. Figure 2(a) shows the Raman spectra of a representative as-deposited nanocrystalline n-type GaN film. The spectrum is dominated by a strong and broad peak located at  $\sim 715 \text{ cm}^{-1}$  with two shoulders at  $\sim 587$  and  $\sim 485 \text{ cm}^{-1}$ . When the peak at  $\sim 715 \text{ cm}^{-1}$  is deconvoluted, one may observe (inset of figure 2(a)) that the peak may be resolved into three peaks located at  $\sim 717$ ,  $\sim 586$  and  $\sim 486 \text{ cm}^{-1}$ . The peak  $\sim 717 \text{ cm}^{-1}$  may be identified as arising from  $A_1$  (LO) phonons in h-GaN while the peak  $\sim 586 \text{ cm}^{-1}$  matches well with the high frequency  $E_2$  (TO) mode of h-GaN [15, 16]. The Raman peak  $\sim 486 \text{ cm}^{-1}$  may be due to vacancy related defects arising out of incorporation of silicon in h-GaN. It may be mentioned here that a-Si indicated a strong Raman line at  $\sim 480 \text{ cm}^{-1}$  for transverse optical phonons [17].

### 3.3. FTIR studies

A FTIR spectrum for a representative n-GaN film is shown in figure 2(b). It may be noted that the spectrum is dominated by strong peaks at  $\sim 611 \text{ cm}^{-1}$  followed by peaks at  $\sim 735$ ,  $1106$  and  $1421 \text{ cm}^{-1}$ . The peak  $\sim 611 \text{ cm}^{-1}$  is broad and

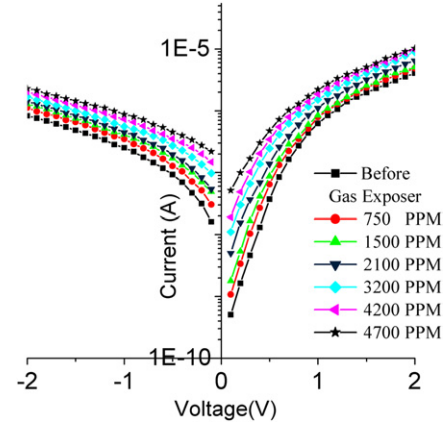


**Figure 3.** Variation of current ( $I$ ) with applied voltage ( $V$ ) measured at room temperature for a representative Al/n-GaN/Pd Schottky diode before and after gas exposure.

has a shoulder at  $\sim 565 \text{ cm}^{-1}$ . Upon de-convolution (inset of figure 2(b)), one may observe that this peak consists of two peaks located at  $\sim 570$  and  $613 \text{ cm}^{-1}$  which may be ascribed to the stretching mode of Ga–N and Ga–O–Ga stretching modes arising due to physisorption of oxygen at the nanocrystalline GaN film. The peak at  $\sim 735 \text{ cm}^{-1}$  is also a typical signature of Ga–O–Ga stretching modes. Boo *et al* [18] indicated that peaks for Ga–N stretching modes might appear between  $550$  and  $573 \text{ cm}^{-1}$  while peaks arising out of Ga–O–Ga modes may appear between  $679$  and  $745 \text{ cm}^{-1}$  [19]. Thus our observation is in good agreement with that obtained by them. The absorption peaks at  $\sim 1106$  and  $1421 \text{ cm}^{-1}$  are due to Si–O bonds originating from the substrate (silicon) used for recording the FTIR in transmission mode.

### 3.4. Al/n-GaN/Pd Schottky diodes

**3.4.1.  $I$ – $V$  measurements.** The primary conduction mechanism in Schottky diodes, in general, is due to the flow of majority charge carriers over the barrier by a thermionic process. The electrical characterization of a Schottky diode necessitates the determination of the barrier height and the ideality factor. For an ideal diode, the diode quality factor ( $n$ ) should be nearly equal to unity. But in a real situation, it may increase when the effects of series resistance, leakage current, etc come into play. The current–voltage ( $I$ – $V$ ) plots measured at  $300 \text{ K}$  for a representative Al/n-GaN/Pd Schottky diode before and after exposure to different hydrogen concentrations are shown in figure 3.

Depending on the temperature ( $T$ ) and applied voltage ( $V$ ), different transport mechanisms may be simultaneously operative in the Schottky diode modulating the charge transport. Assuming that the thermionic emission is the most predominant mechanism, the general form of the temperature dependence of current may now be expressed as [20]

$$I = AA^*T^2 \exp(-\beta\Phi_B) \exp\left[\frac{\beta(V - IR)}{n}\right], \quad (1)$$

where  $\Phi_B = (\varphi_B - \Delta\varphi_B)$  is the effective barrier height,  $\Delta\varphi_B$  corresponds to the barrier height lowering,  $A$  is the junction area,  $A^*$  ( $A^* = 4\pi qm^*k^2/h^3$ ) is the Richardson constant and

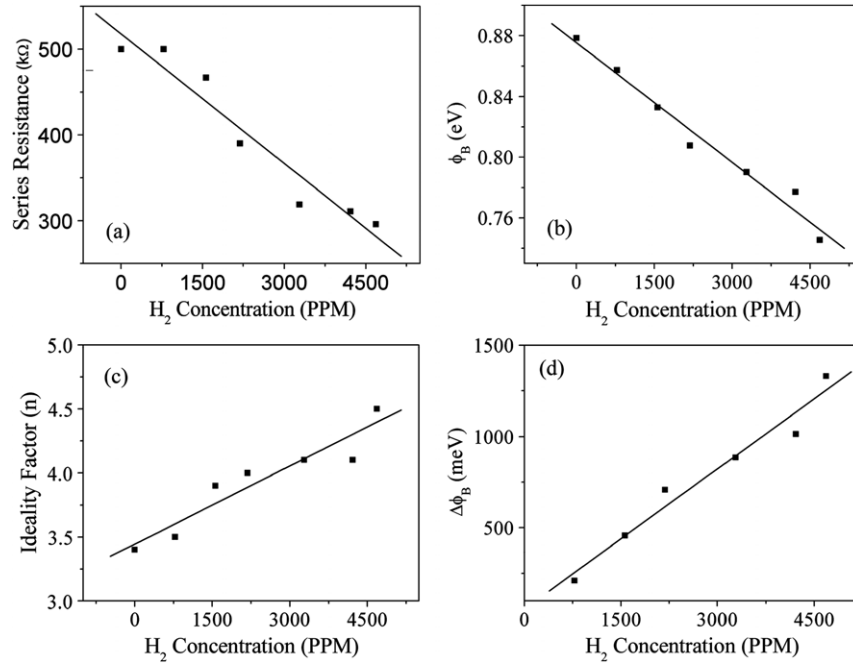


**Figure 4.** Variation of (a) series resistance, (b) barrier potential ( $\phi_B$ ), (c) ideality factor ( $n$ ) and (d)  $\Delta\phi_B$  with different  $H_2$  concentrations for Al/n-GaN/Pd Schottky diode.

$m^*$  is the effective mass of the charge carriers.  $R$  is the series resistance and  $\beta = q/kT$ .

There are inherent difficulties when the base material would offer a high series resistance, which would cause a voltage drop across the junction. Nanocrystalline GaN being a high resistive material would be supposed to offer a high series resistance. A generalized Norde method was used [21, 22] to evaluate the effective barrier height, series resistance and diode ideality factor ( $n$ ) from  $I$ - $V$  measurement. The Norde function,  $F(V)$ , is given by [23]

$$F(V) = \frac{V}{2} - \frac{1}{\beta} \left[ \ln \left( \frac{I}{AA^*T^2} \right) \right]. \quad (2)$$

Bohlin [22] modified the above expression by considering the effect of a high value of series resistance. The effective barrier height, series resistance and ideality factor were evaluated by using the method proposed by Bohlin.

The values of series resistance, effective barrier potential and diode ideality factor measured at different hydrogen concentration at room temperature determined as above for an Al/n-GaN/Pd Schottky diode are shown in figures 4(a)–(c) respectively. The series resistance evaluated from  $I$ - $V$  curves for Al/n-GaN/Pd Schottky diodes measured at 300 K before gas exposure and after gas exposure were  $\sim 500$  k $\Omega$  and  $\sim 300$  k $\Omega$ , respectively. The barrier height could be seen to decrease with hydrogen concentration (figure 4(b)). The difference in Schottky barrier height ( $\Delta\phi_B$ ) on hydrogen exposure relative to that without hydrogen exposure showed linear increase (figure 4(d)) with hydrogen concentration. It may be observed that the ideality factor for the Schottky diodes varied between 3.4 and 4.5, which is comparable [24–26] or higher [21, 27] than those obtained for junctions made out of epilayers. This may be due to the existence of a large number of surface states characterizing the nanolayers constituting the diodes. Ideality

factor increased with hydrogen exposure while it decreased as the temperature was increased (discussed later) at all hydrogen concentrations. The higher value of series resistance obtained here may be due to very high resistance of the n-GaN layer as well as due to the technique adopted here for the fabrication of the diodes.

Temperature dependence of the  $I$ - $V$  characteristics in the forward bias regime for a representative Al/n-GaN/Pd Schottky diode before and after hydrogen gas exposure at different concentrations is shown in figures 5(a)–(c). Variation of the barrier height ( $\phi_B$ ) with temperature of an Al/n-GaN/Pd Schottky diode before and after gas exposure at two representative hydrogen concentrations is shown in figure 6(a). The barrier height could be seen to decrease significantly (figure 4(b)) with increased hydrogen concentration while it increased with temperature (figure 6(a)). The ideality factor decreased with increased temperature at all hydrogen concentration (figure 6(b)).

The sensitivity ( $S$ ) is defined as [6]

$$S = (I_G - I_{Ar})/I_{Ar}, \quad (3)$$

where  $I_G$  and  $I_{Ar}$  are current in hydrogen containing ambient and argon ambient. It may be noted that the above expression may be used for both the forward and reverse current modes at a fixed applied voltage. Figure 7(a) shows the variation of sensitivity with  $H_2$  concentration at room temperature in the forward ( $S_F$ ) and reverse current modes ( $S_R$ ) for a representative GaN film recorded at 3 V. Figures 7(b) and (c) show the variation of sensitivity with operating temperature in forward and reverse current modes, respectively, for two representative hydrogen concentrations. One may observe (figure 7(a)) that the sensitivity increased nearly linearly with hydrogen concentration for both the forward and reverse current modes. It may also be observed that the sensitivity



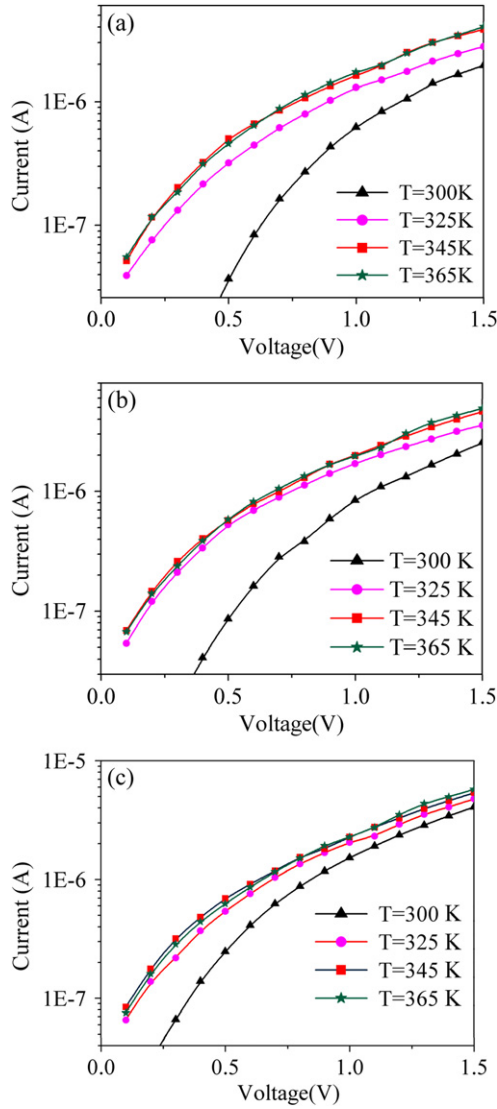


**Figure 5.** Ln  $I$ – $V$  plot (in the forward bias regime) measured at different temperatures for Al/n-GaN/Pd Schottky diode: (a) before gas exposure; after gas exposure (b) at 1500 ppm and (c) 3200 ppm.

showed a decrease with increasing temperature for both the forward and reverse current modes. This might be due to desorption of hydrogen as the temperature was increased.

Figure 8 represents the variation of sensitivity with time measured at room temperature (300 K) as the test gas (hydrogen at 3200 ppm) is introduced in the chamber. It may be seen that the maximum sensitivity could be attained in less than 15 min. After withdrawal of the test gas, the sensor tends to come back to near initial state and this change is exponential. Sensitivity decreases for the next 50 min and then tends to come back to the original state slowly. The response time for Pd/GaN Schottky diode reported by Huang *et al* [13] was  $\sim 66$  min while that for Pt/GaN Schottky diode as reported by Ali *et al* [3] was  $\sim 76$  min. Thus, the response time of the Schottky diode sensor studied here is superior to those reported recently by other workers [3, 13]. It may be noted here that the Schottky diodes used by them are based on epilayers of GaN deposited by metal organic chemical vapour deposition (MOCVD). The

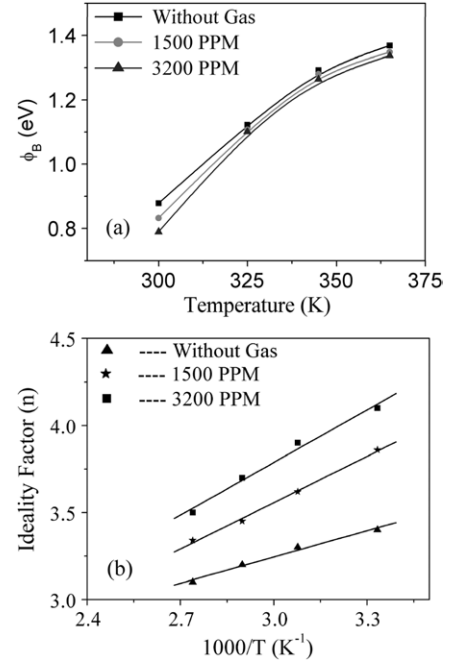


**Figure 6.** Variation of (a) barrier potential ( $\phi_B$ ) and (b) ideality factor ( $n$ ) with the temperature before and after gas exposure (for two representative  $H_2$  concentrations).

response time defines the time taken for the sensor to reach 90% of the saturation value after contact of the test gas with the surface of the sensor. The above observation suggests that the response time in these films would be  $\sim 12$  min.

The modulation of barrier height with exposure to hydrogen gas leading towards the possible use of the Al/n-GaN/Pd Schottky diode as a hydrogen gas sensor may be understood from the following considerations. It is generally accepted that dissociative adsorption of diatomic hydrogen molecules at Pd surface would need the formation of transient active sites for dissociative adsorption of  $H_2$  molecules. Mitsul *et al* [28] reported from their study by scanning tunneling microscopy that three or more vacancy aggregates are needed for efficient hydrogen dissociation. The top palladium contact is obtained by evaporating Pd film and as such these palladium films would contain large numbers of defects, which may be conducive to the formation of such vacancy aggregates for dissociative hydrogen adsorption. These hydrogen atoms would then diffuse through the thin Pd film and come in contact with the Pd/GaN interface [29, 30] and get polarized to form a dipolar layer near the interface. Once the dipolar layer is formed at the interface, there would be a tendency for the electrostatic potential of GaN to shift, that would culminate in a significant decrease in Schottky barrier height. This decrease in barrier height would be in proportion to hydrogen concentration. This observation is commensurate with what is reported in this communication. At this juncture it may be worth noting that Cabrera *et al* [31] observed that with the exposure to hydrogen, the resistance of a Pd layer increases with increasing amount of hydrogen and could be correlated with the presence of  $\alpha$ -phase of Pd hydrides [32]. The equilibrium solubility isotherm of  $PdH_x$  was obtained around 307 K and  $x$  changed continuously from 0 to 0.15 with hydrogen pressure. Thus, increased resistance of the Pd layer

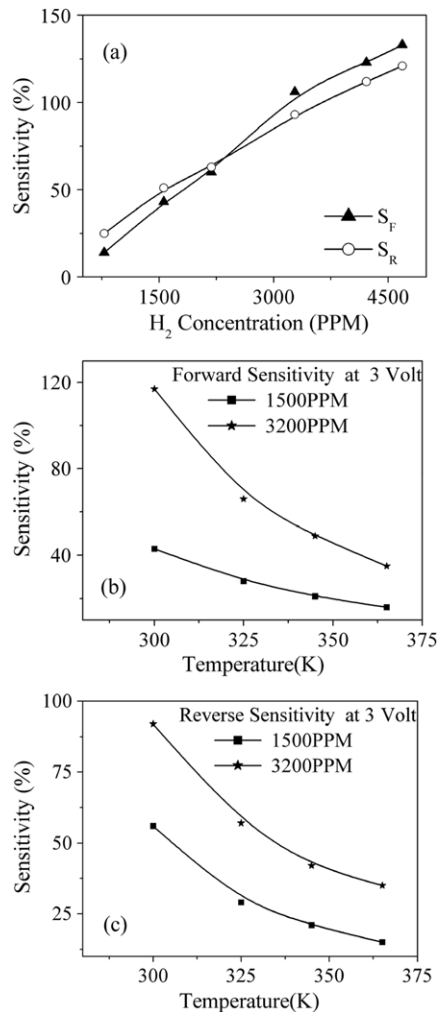


**Figure 7.** Variation of sensitivity with: (a) hydrogen concentration measured at 3 V for a representative film in the forward current and reverse current, (b) temperature (in K) for two representative hydrogen concentrations in the forward current mode and (c) in reverse current mode.

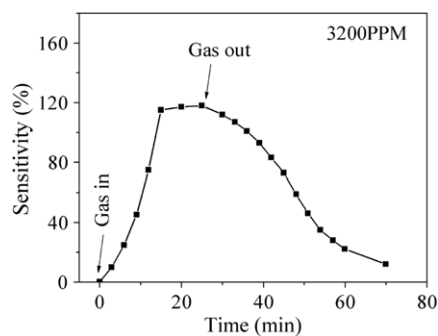


**Figure 8.** Response behaviour of a representative Al/n-GaN/Pd Schottky diode sensor.

would also contribute to the lowering of Schottky barrier height in these Al/n-GaN/Pd Schottky diodes studied here.

The linear dependence of ideality factor  $n$  with inverse of temperature may be observed (figure 6(b)) for the diodes on exposure to hydrogen. Generally, the variation of  $n$  with temperature ( $T$ ) is expressed as [33]

$$n = A + B/T. \quad (4)$$

The values of  $A$  and  $B$  for the n-GaN/Pd Schottky diodes before and after gas exposure may be obtained from the intercept and the slope, respectively, of the straight-line plot of  $n$  versus  $1/T$  (figure 6(b)). The value of  $A$  decreased from 1.73 to 0.76 with increasing amount of hydrogen while the  $B$  value indicated an increase from 500 to 1000 K with increasing amount of hydrogen. It was also observed that the ideality factor ( $n$ ) was found to decrease while the barrier height ( $\phi_B$ ) increased with temperature at all hydrogen exposure. This may be due to the temperature activated process modulating the current transport across metal/semiconductor interface. Electrons will be able to surmount the lower barrier height at lower temperatures through the zones having lower barrier height and higher ideality factor at the interface. With the increase in temperature, electrons will have enhanced energies to surmount higher barrier height. The above effect could be attributed to inhomogeneous interfaces and barrier heights due to the linear relationship between the barrier height and ideality factor. This may be commensurate with the observation of decreasing barrier height with hydrogen exposure culminating in a dipolar layer at the interface. This would shift the electrostatic potential of GaN resulting in a significant decrease in Schottky barrier height. This decrease in barrier height would be in proportion to hydrogen concentration as has been observed here. Also the resistance of the Pd layer would increase with the formation of high resistive  $\alpha$ -phase of Pd hydrides contributing to the lowering of Schottky barrier height with exposure to hydrogen.

#### 4. Conclusion

Schottky diode structures, Al/n-GaN/Pd, were realized by depositing nanocrystalline n-GaN (1 at% Si) layers onto aluminium coated fused silica substrate by a high pressure sputtering technique. The  $I$ - $V$  characteristic of the above Schottky diode was measured at different temperatures before and after hydrogen gas exposure. The series resistances evaluated from the room temperature (300 K)  $I$ - $V$  curves for the Al/n-GaN/Pd Schottky diode before and after hydrogen gas exposure were  $\sim 500$  and  $\sim 300$  k $\Omega$ . The ideality factor for the Schottky diodes varied between 3.4 and 4.5. The barrier height could be seen to decrease significantly with increased hydrogen concentration while it increased with temperature. The ideality factor ( $n$ ) was found to decrease while the barrier height ( $\phi_B$ ) increased with temperature at all hydrogen exposures. This may be due to the temperature activated process modulating the current transport across metal/semiconductor interface.

#### Acknowledgments

The authors wish to thank the Department of Science and Technology, Government of India, for sanctioning financial assistance for executing this programme. SND wishes to acknowledge with thanks the award of a fellowship to him by the Coal S & T, Government of India.

#### References

- [1] Deshpande S, Seal S, Zhang P, Cho H J and Posey N 2007 *Appl. Phys. Lett.* **90** 073118

- [2] Yam F K, Hassan Z and Hudeish A Y 2007 *Thin Solid Films* **515** 7337
- [3] Ali M, Cimalla V, Lebedev V, Romanus H, Tilak V, Merfield D, Sandvik P and Ambacher O 2006 *Sensors Actuators B* **113** 797
- [4] Han C H, Hong D W, Han S D, Gwak J and Singh K C 2007 *Sensors Actuators B* **125** 224
- [5] Lee D S, Lee J H, Lee Y H and Lee D D 2003 *Sensors Actuators B* **89** 305
- [6] Song J, Lu W, Flynn J S and Brandes G R 2005 *Appl. Phys. Lett.* **87** 133501
- [7] Spetz A L *et al* 2001 *Phys. Status Solidi a* **185** 15
- [8] Tobias P, Baranzanhi A, Spetz A L, Kordina O, Janzen E and Lundstorm I 1997 *IEEE Electron Dev. Lett.* **18** 287
- [9] Osinski M 2002 *Gallium-Nitride-Based Technologies* (Washington, DC: SPIE)
- [10] Huang H W, Chu J T, Kao C C, Hseuh T H, Lu T C, Kuo H C, Wang S C and Yu C C 2005 *Nanotechnology* **16** 1844
- [11] Schubert E F 2003 *Light-Emitting Diodes* (Cambridge: Cambridge University Press)
- [12] Hasegawa S, Nishida S, Yamashita T and Asahi H 2005 *Thin Solid Films* **487** 260
- [13] Huang J-R, Hsu W-C, Chen H-I and Liu W-C 2007 *Sensors Actuators B* **123** 1040
- [14] Das S N and Pal A K 2006 *Semicond. Sci. Technol.* **21** 1557
- [15] Murugkar S, Merlin R, Botchkarev A, Salvador A and Morkoc H 1995 *J. Appl. Phys.* **77** 6042
- [16] Kozawa T, Kachi T, Kano H, Taga Y, Hashimoto M, Koide N and Manabe K 1994 *J. Appl. Phys.* **75** 1098
- [17] Brodsky M H, Cardona M and Cuomo J J 1997 *Phys. Rev. B* **16** 3556
- [18] Boo J, Rohr C and Ho W 1998 *J. Cryst. Growth* **189–190** 439
- [19] Lee D S and Steckl A J 2001 *Appl. Phys. Lett.* **79** 1962
- [20] Sze S M 1979 *Physics of Semiconductor Devices* (New Delhi: Wiley Eastern Limited)
- [21] Noh S K and Bhattacharya P 2001 *Appl. Phys. Lett.* **78** 3642
- [22] Bohlin K E 1986 *J. Appl. Phys.* **60** 1223
- [23] Norde H 1979 *J. Appl. Phys.* **50** 5052
- [24] Shah J M, Li Y L, Gessmann T and Schubert E F 2003 *J. Appl. Phys.* **94** 2627
- [25] Colder H, Rizk R, Pichon L and Bonnaud O 2006 *Solid State Electron.* **50** 209
- [26] Osvald J, Kuzmik J, Konstantinidis G, Lobotka P and Georgakilas A 2005 *Microelectron. Eng.* **81** 181
- [27] Akkal B, Benamarara Z, Abid H, Talibi A and Gruzza B 2004 *Mater. Chem. Phys.* **85** 27
- [28] Mitsul T, Rose M K, Fomin F, Ogletree D F and Salmeron M 2003 *Nature* **422** 705
- [29] Schalwig J, Muller G, Karrer U, Eickhoff M, Ambacher O, Stutzmann M, Gorgens L and Dollinger G 2002 *Appl. Phys. Lett.* **80** 1222
- [30] Lundstrom I and Petersson L G 1996 *J. Vac. Sci. Technol. A* **14** 1539
- [31] Cabrera A L and Aguayo-Soto R 1997 *Catal. Lett.* **45** 79
- [32] Frieske H and Wicke E 1973 *Phys. Chem.* **77** 48
- [33] Ozdemir S and Altindal S 1994 *Solar Energy Mater. Solar Cells* **32** 115